oxidative electrolysis of the solution at 0.8 V, the initially yellow solution turned blue, then gradually dark red, and finally yellow. This color change corresponds to the oxidation of yellow $[Pt_2(NH_3)_4(C_4H_6NO)_2]^{2+}$ to blue $[Pt_4(NH_3)_8(C_4H_6NO)_4]^{5+}$ and dark red $[Pt_4(NH_3)_8(C_4H_6NO)_4]^{6+}$ and finally to yellow $[Pt_4(NH_3)_8(C_4H_6NO)_4]^{8+}$,[22] which was confirmed by UV-visible absorption spectra. Bulk coulometry of the solution shows that the single wave at 0.53 V corresponds to a 4-electron redox process as a whole. The peak separation between E_{pc} and E_{pa} in the cyclic voltammogram could not be decreased less than 0.07 V at any scan rate from 0.001 to 0.5 V s^{-1}. A separate electrochemical study of $[Pt_4(NH_3)_8(C_4H_6NO)_4]^{6+}$ shows the cation also undergoes a single redox process at 0.53 V.[23] These facts, together with the color change during the bulk electrolysis of $[Pt_2(NH_3)_4(C_4H_6NO)_2]^{2+}$ and the very rapid isomerization from H-H to H-T, suggest that the redox reaction of $[Pt_2(NH_3)_4(C_4H_6NO)_2]^{2+}$ at 0.53 V is irreversible and consists actually of two or more very closely lying processes. The appearance of blue color in the bulk oxidative electrolysis signifies that at least the first oxidative step would be a 1- or 2-electron process

$$[Pt_2(NH_3)_4(C_4H_6NO)_2]^{2+} \xrightarrow{-e^-} [Pt_2(NH_3)_4(C_4H_6NO)_2]^{3+}$$

or

$$[Pt_2(NH_3)_4(C_4H_6NO)_2]^{2+} \xrightarrow{-2e^-} [Pt_2(NH_3)_4(C_4H_6NO)_2]^{4+}$$

The blue $[Pt_4(NH_3)_8(C_4H_6NO)_4]^{5+}$ cation would be formed by either one of the two following reactions:

$$[Pt_2(NH_3)_4(C_4H_6NO)_2]^{3+} + [Pt_2(NH_3)_4(C_4H_6NO)_2]^{2+} \rightarrow [Pt_4(NH_3)_8(C_4H_6NO)_4]^{5+}$$

$$[Pt_2(NH_3)_4(C_4H_6NO)_2]^{4+} + 3[Pt_2(NH_3)_4(C_4H_6NO)_2]^{2+} \rightarrow 2[Pt_4(NH_3)_8(C_4H_6NO)_4]^{5+}$$

It seems that H-H and H-T $[Pt_2(NH_3)_4(C_4H_6NO)_2]^{2+}$ isomers have very close or almost identical redox potentials or oxidation of either isomer triggers very rapid isomerization and the oxidation proceeds almost exclusively via either one of the isomers. It also seems that some isomerization occurs following oxidation of the compound, since the cyclic voltammogram becomes less reversible with the peak separation between E_{pa} and E_{pc} being increased, though the E_p potential is retained, as the acidity of the solution is decreased.

Conclusion

Lippard et al. reported a possible relationship between structural features, such as the Pt-Pt distance and the torsional angle about the Pt-Pt vector, and the ease of linkage isomerization.[4] The long Pt-Pt distance in the present complex may result in the rapid isomerization of the complex. However, the torsional angle in this complex is not so large; therefore, it seems that rapid isomerization does not always result from strong torsional strain. The isomerization seems also to be related to the nature of the amide ligand. The relative contributions of the keto and enol forms of the amidate ligand influence the relative degrees of the coordinating abilities of amidate oxygen and nitrogen atoms and thus affect the isomerization rate.

The present study clarified the solid and solution structures of a *cis*-diammineplatinum(II) α-pyrrolidonate complex, which was synthesized by the reduction of the tetranuclear Pt(II) and Pt(III) mixed-valent complex $[Pt_4(NH_3)_8(C_4H_6NO)_4]^{6+}$.

Acknowledgment. We are indebted to the Toray Science Foundation and Japanese Ministry for Health and Welfare for their financial support.

Registry No. $[Pt_2(NH_3)_4(C_4H_6NO)_2]_2(PF_6)_3(NO_3)\cdot H_2O$, 119942-98-2; ^{195}Pt, 14191-88-9.

Supplementary Material Available: Anisotropic thermal parameters (Table S2) (1 page); final observed and calculated structure factors (Table S1) (19 pages). Ordering information is given on any current masthead page.

Contribution from the Departments of Chemistry, Queens College-City University of New York, Flushing, New York 11367-0904, and University of Houston, Houston, Texas 77204-5641

Resonance Raman Spectra and Excited-State Lifetimes for a Series of 3,3′-Polymethylene-2,2′-bipyridine Complexes of Ruthenium(II)

Thomas C. Strekas,*,† Harry D. Gafney,† Steven A. Tysoe,† Randolph P. Thummel,*,‡ and Francois Lefoulon‡

Received December 6, 1988

The complexes RuL_3^{2+}, where L is a 3,3′-polymethylene-2,2′-bipyridine ligand containing one to four bridging methylene units, were studied by using resonance-enhanced Raman spectroscopy. Lifetimes and emission spectra were measured at room temperature and at 77 K. Complexes with the monomethylene-bridged ligand show results distinctly different from those of the dimethylene-, trimethylene-, and tetramethylene-bridged ligand complexes, which form a series showing systematic variations in the resonance Raman and emission spectra that correlate with the degree to which the polymethylene bridge distorts the planarity of 2,2′-bipyridine. As the bridge length increases, the relative quantum yield for emission at 25 °C drops. Twisting about the 2,2′-bond may result in a weakening of the ligand field leading to lower lying ligand field states, which provide a route for more facile radiationless deactivation. Both the relative intensity pattern in the resonance Raman spectra and the intensities of the low-energy shoulders in the 77 K emission spectra suggest an increase in the number of ligand normal modes capable of efficiently coupling ground and excited states as the number of methylene units increases from 2 to 4. This is consistent with increased rates for nonradiative deexcitation, most likely through these same high-frequency "acceptor" modes.

Introduction

The effect of varying steric and electronic factors in diimine type ligands on the properties of their ruthenium(II) complexes remains an active area of investigation.[1] Because of the capability of $Ru(bpy)_3^{2+}$ (bpy = 2,2′-bipyridine) to act as an excited-state redox reagent,[2] the degree to which ligand properties can influence the excited-state properties of these complexes is of considerable interest.

Recently reported[3] NMR and X-ray data concerning the ruthenium(II) complexes of a series of 3,3′-polymethylene-bridged

† Queens College.
‡ University of Houston.

(1) (a) Thummel, R. P.; Lefoulon, F. *Inorg. Chem.* **1987**, *26*, 675. (b) Thummel, R. P.; Decloitre, Y.; Lefoulon, F. *Inorg. Chim. Acta* **1987**, *128*, 245. (c) Binamira-Soriga, E.; Sprouse, S. D.; Watts, R. J.; Kaska, W. C. *Inorg. Chim. Acta* **1984**, *84*, 135. (d) Klassen, D. M. *Inorg. Chem.* **1976**, *15*, 3166. (e) Anderson, S.; Seddon, K. R.; Wright, R. D. *Chem. Phys. Lett.* **1980**, *71*, 220. (f) Allen, G. H.; White, R. P.; Rillema, D. P.; Meyer, T. *J. Am. Chem. Soc.* **1984**, *106*, 2613. (g) Balzani, V.; Juris, A.; Barigelletti, F.; Belser, P.; von Zelewsky, A. *Sci. Pap. Inst. Phys. Chem. Res. (Jpn.)*. **1984**, *78*, 78. (h) Belser, P.; von Zelewsky, A. *Helv. Chim. Acta.* **1980**, *63*, 1675. (i) Belser, P.; von Zelewsky, A. *Chem. Phys. Lett.* **1982**, *89*, 101.

0020-1669/89/1328-2964$01.50/0

2,2'-bipyridines (**1a–d**) indicate that this series provides a well-defined set of structurally similar tris complexes which vary with respect to the dihedral angle defined by the halves of the bipyridine ligand. The widest variation in properties was found for the

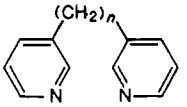

1a, $n = 1$
b, $n = 2$
c, $n = 3$
d, $n = 4$

luminescence intensity in fluid solution at room temperature. For $Ru(\mathbf{1a})_3^{2+}$ no luminescence was detected, as previously reported.[4] For $Ru(\mathbf{1b})_3^{2+}$ luminescence was comparable to that of $Ru(bpy)_3^{2+}$, for $Ru(\mathbf{1c})_3^{2+}$ it was reduced by about 1 order of magnitude, and for $Ru(\mathbf{1d})_3^{2+}$ it was barely detectable and was red-shifted with a maximum at about 680 nm.

Resonance-enhanced Raman spectroscopy of ruthenium(II) diimine complexes[5] has played an important role in elucidating both ground- and excited-state properties of these molecules. Vibrational frequencies yield information about the ground-state geometries of the coordinated ligands, while intensities can be indicative of the specific normal modes that are most efficient in coupling[6] the ground and excited states during absorption, and also during emission, if one can assume that the emissive and absorptive excited states are similar. We therefore have recorded the resonance Raman spectra of the series of complexes $Ru(\mathbf{1a–d})_3^{2+}$ using excitation near the peak of the visible metal-to-ligand charge-transfer (MLCT) absorption. The results provide the basis for a confirmation of the degree of structural variation of the coordinated ligands **1a–d** as the bridge length varies, as well as an indication of the changing character of the normal modes most efficient in vibronically coupling the ground and excited states in absorption. In addition, we report lifetime measurements at room temperature in solution and at 77 K for the series.

Experimental Section

The complexes were prepared and purified as previously reported.[3a] For Raman spectroscopy, solutions were prepared in acetonitrile at metal complex concentrations of about 10^{-4} M. Absorption spectra were recorded with a Perkin-Elmer Lambda 3 spectrophotometer to determine concentrations. Emission spectra and lifetimes were measured with use of dilute ($\sim 10^{-5}$ M) solutions in acetonitrile. For lifetime measurements, the solutions were deaerated by flushing with dry nitrogen.

Resonance Raman spectra at room temperature were obtained with a Spectra-Physics Model 164-08 argon ion laser. Scattered light was collected at 90° and dispersed by the first half of a SPEX 14018 double monochromator. A Princeton Instruments OSMA system with an ST-100 detector controller and an IRY700G microchannel plate image intensified photodiode array was used to collect and process the signal at this point. The spectra were calibrated with use of toluene as a wavelength standard.

Emission spectra at both room and liquid-nitrogen temperature were recorded on a Perkin-Elmer Hitachi MPF-2A spectrophotometer. Lifetimes were measured with a Quanta-Ray DCR-2A Nd:YAG laser as the excitation source and a Bausch & Lomb 33-86-76 monochromator to disperse the 90° scattered light. Detection was accomplished with an RCA C31034 PMT connected to a Tektronix 7834 oscilloscope.

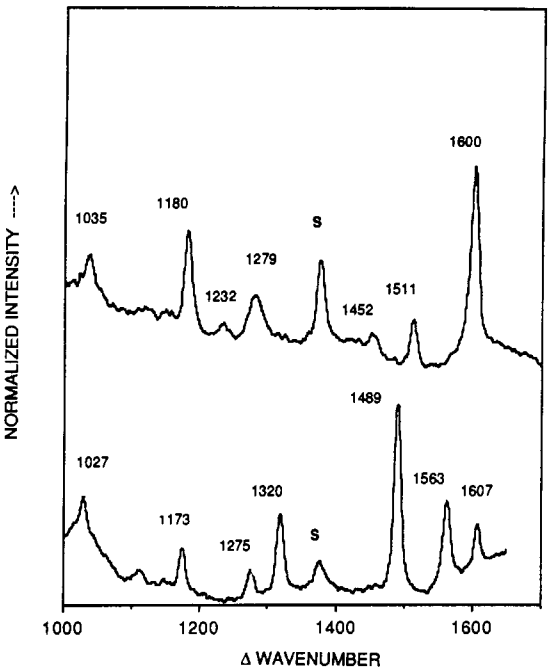

Figure 1. Resonance Raman spectra of $Ru(bpy)_3^{2+}$ (bottom) and $Ru(\mathbf{1a})_3^{2+}$ (top) at room temperature in acetonitrile solution at $\sim 10^{-4}$ M (excitation wavelength 457.9 nm). The spectra have been normalized to the peak height of the most prominent peak to facilitate relative intensity comparisons.

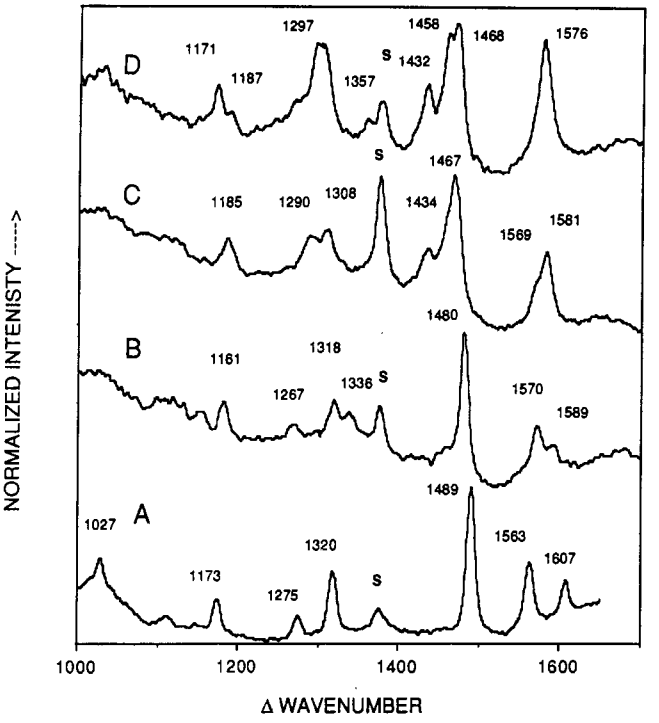

Figure 2. Resonance Raman spectra of $Ru(bpy)_3^{2+}$ (A), $Ru(\mathbf{1b})_3^{2+}$ (B), $Ru(\mathbf{1c})_3^{2+}$ (C), and $Ru(\mathbf{1d})_3^{2+}$ (D) at room temperature in acetonitrile solution at $\sim 10^{-4}$ M (excitation wavelength 457.9 nm). The spectra have been normalized to the peak height of the most prominent peak to facilitate relative intensity comparisons.

(2) (a) Watts, R. J. *J. Chem. Educ.* **1983**, *60*, 834. (b) Kalyanasundaram, K. *Coord. Chem. Rev.* **1982**, 159.
(3) (a) Thummel, R. P.; Lefoulon, F.; Korp, J. D. *Inorg. Chem.* **1987**, *26*, 2370. (b) Thummel, R. P.; Lefoulon, F.; Mahadevan, R. *J. Org. Chem.* **1985**, *50*, 3824.
(4) Henderson, L. J.; Fronczek, F. R.; Cherry, W. R. *J. Am. Chem. Soc.* **1984**, *106*, 5876.
(5) (a) Fuchs, Y.; Lofters, S.; Dieter, T.; Shi, W.; Morgan, R.; Strekas, T. C.; Gafney, H. D.; Baker, A. D. *J. Am. Chem. Soc.* **1987**, *109*, 2691. (b) Wolfgang, S.; Strekas, T. C.; Gafney, H. D.; Krause, R.; Krause, K. *Inorg. Chem.* **1984**, *23*, 2650. (c) Knors, C.; Gafney, H. D.; Baker, A. D.; Braunstein, C. H.; Strekas, T. C. *J. Raman Spectrosc.* **1983**, *14*, 32. (d) Chung, Y. C.; Leventis, N.; Wagner, P. J.; Leroi, G. E. *J. Am. Chem. Soc.* **1985**, *107*, 1414. (e) Smothers, W. K.; Wrighton, M. S. *J. Am. Chem. Soc.* **1983**, *105*, 1067. (f) Bradley, P. G.; Kress, N.; Hornberger, B. A.; Dallinger, R. F.; Woodruff, W. H. *J. Am. Chem. Soc.* **1979**, *101*, 4391. (g) Caswell, D. S.; Spiro, T. G. *Inorg. Chem.* **1987**, *26*, 18. (h) McClanahan, S.; Kincaid, J. *J. Raman Spectrosc.* **1984**, *15*, 173. (i) Tait, C. D.; MacQueen, D. B.; Donohoe, R. J.; DeArmond, M. K.; Hanck, K. W.; Wertz, D. W. *J. Phys. Chem.* **1986**, *90*, 1766.
(6) (a) Kober, E. M.; Meyer, T. J. *Inorg. Chem.* **1985**, *24*, 106. (b) Caspar, J. V.; Westmoreland, T. D.; Allen, G. H.; Bradley, P. G.; Meyer, T. J.; Woodruff, W. H. *J. Am. Chem. Soc.* **1984**, *106*, 3492.
(7) Zerbi, G.; Sandroni, S. *Spectrochim. Acta, Part A* **1968**, *24A*, 511.

Table I. Measured Lifetimes for RuL_3^{2+} Complexes (L = bpy, **1a–d**) at 25 °C and 77 K

complex	liq soln, ns[a]	frozen soln, μs[b]	complex	liq soln, ns[a]	frozen soln, μs[b]
$Ru(bpy)_3^{2+}$	620	5.3	$Ru(\mathbf{1c})_3^{2+}$	455	2.7
$Ru(\mathbf{1a})_3^{2+}$	*c*	5.5	$Ru(\mathbf{1d})_3^{2+}$	*d*	3.6[e]
$Ru(\mathbf{1b})_3^{2+}$	630	5.4			

[a] Approximately 10^{-5} M solutions in acetonitrile at 25 °C. [b] Same as in *a*, but frozen solutions in cold finger Dewar at 77 K. [c] No emission observed. [d] Signal too weak to measure lifetime at reported 680-nm emission maximum. [e] Maximum at 77 K is 606 nm.

Results

In Figures 1 and 2, the resonance-enhanced Raman spectra from 1000 to 1700 cm^{-1}, obtained with 457.9-nm excitation, are displayed for acetonitrile solutions of the four tris complexes of Ru(II) with **1a–d**, as well as $Ru(bpy)_3^{2+}$. Figure 1 compares the spectrum for $Ru(\mathbf{1a})_3^{2+}$ with that of $Ru(bpy)_3^{2+}$, while Figure 2 compares the spectra of the tris complexes of the other three bridged ligands with that of $Ru(bpy)_3^{2+}$. The 457.9-nm excitation corresponds closely to the MLCT maximum for all the complexes and provides the maximum resonance enhancement in each case. As previously reported,[3a] the visible MLCT transition maxima of the bridged ligand complexes fall within the range 437–462 nm, each with a shoulder 5–10 nm to the blue. Other usable argon ion excitation lines available in our laboratory (e.g. 488.0 nm) produce essentially identical resonance-enhanced spectra. The 1374-cm^{-1} band of the solvent acetonitrile serves as an internal intensity marker, demonstrating that for all complexes the resonance Raman enhancement with 457.9-nm excitation is comparable.

Emission spectra of all five complexes at 77 K are presented in Figure 3. In order to facilitate discussion of the nature of the low-frequency shoulder seen in each spectrum, the emission intensities are normalized to the same arbitrary scale. The results of lifetime measurements are displayed in Table I.

Discussion

Inspection of the resonance-enhanced Raman vibrational spectra (Figure 2) indicates a continuous change in pattern with increase in the number of bridging methylene groups from $Ru(bpy)_3^{2+}$ to $Ru(\mathbf{1d})^{32+}$ with the exception of the spectrum of $Ru(\mathbf{1a})_3^{2+}$ (Figure 1), which is distinct from the others. Leaving this latter spectrum aside, note the correspondence of the bands at 1607 and 1563 cm^{-1} in the bpy complex spectrum (bottom of Figure 2) to a shifted pair at 1589 and 1570 cm^{-1} in the spectrum of $Ru(\mathbf{1b})_3^{2+}$ to a peak at 1581 cm^{-1} with a 1569-cm^{-1} shoulder in the spectrum of $Ru(\mathbf{1c})_3^{2+}$, and finally to a single peak at 1576 cm^{-1} in the $Ru(\mathbf{1d})_3^{2+}$ spectrum (probably two unresolvable bands). The prominent 1489-cm^{-1} bpy band shifts to 1480 cm^{-1} for $Ru(\mathbf{1b})_3^{2+}$ to 1467 cm^{-1}, with asymmetric broadening on the low-frequency side, for $Ru(\mathbf{1c})_3^{2+}$ and finally we see a 1458- and a 1468-cm^{-1} pair for $Ru(\mathbf{1d})_3^{2+}$. The 1275, 1320 cm^{-1} pair for bpy are slightly shifted for the dimethylene-bridged complex, move closer for the trimethylene-bridged one (1290, 1308 cm^{-1}), and coalesce to an unresolved pair at 1297 cm^{-1} for the tetramethylene-bridged complex. The 1173-cm^{-1} bpy band appears to split into two components at 1171 and 1187 cm^{-1} for the tetramethylene-bridged complex, after showing asymmetric broadening to the high-frequency side for the trimethylene-bridged complex. In addition, a new band emerges at 1434 cm^{-1} in the spectrum of $Ru(\mathbf{1c})_3^{2+}$. This band is also seen at 1432 cm^{-1} for $Ru(\mathbf{1d})_3^{2+}$. Finally, the tetramethylene-bridged complex spectrum shows a new band at 1357 cm^{-1} and a low-frequency shoulder on the 1297-cm^{-1} band.

The resonance-enhanced Raman spectrum of $Ru(\mathbf{1a})_3^{2+}$ (Figure 1) serves to emphasize the fact that this complex is distinct from the others, although still related to $Ru(bpy)_3^{2+}$. It shows a set of seven bands that likely correlate one-to-one with the seven bands in the bpy complex spectrum. the five highest frequency bands are downshifted from their bpy counterparts (bpy/**1a**): 1607/1600, 1563/1511, 1489/1452, 1320/1279, 1275/1232 cm^{-1}. The broadening of the 1279-cm^{-1} band is likely due to normal-coordinate mixing of a methylene carbon to ring carbon stretch ($-CH_2-C_3$ ring) with resonance-enhanced ring-stretching modes at nearly the same frequency, thereby creating an additional resonance-enhanced mode. A similar effect is observed in spectra of 4,4′-dimethyl-2,2′-bipyridine complexes of ruthenium(II) and for the rest of the complexes discussed below. The 1173- and 1027-cm^{-1} bands of $Ru(bpy)_3^{2+}$ are found at approximately the same frequency for all complexes reported here. They are assigned[5h] as in-plane C–H deformation mixed with symmetric in-plane ring stretching, involving simultaneous distortion of all ring bonds.

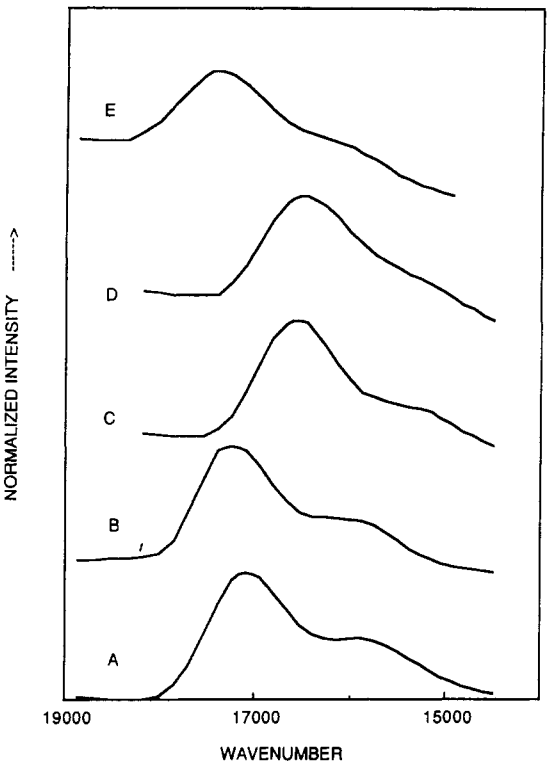

Figure 3. Emission spectra at 77 K of frozen acetonitrile solutions of $Ru(bpy)_3^{2+}$ (A) $Ru(\mathbf{1b})_3^{2+}$ (B), $Ru(\mathbf{1c})_3^{2+}$ (C), $Ru(\mathbf{1d})_3^{2+}$ (D), and $Ru(\mathbf{1a})_3^{2+}$ (E). The data have been normalized to display the same maximum peak intensity for all spectra.

The X-ray structure[3a] of $Ru(bpy)_2(\mathbf{1d})^{2+}$ shows that the dihedral angle between the planes of the two coordinated pyridine rings of **1d** is 30.4°, reduced from an estimated 80° in the free ligand because of the constraints imposed by chelation to the metal. Probably more relevant to a discussion of the vibrational frequencies, the two pyridine rings are found to be significantly distorted from planarity. Structures for the other complexed methylene-bridged ligands are not available, but interpretation of NMR data indicates that there is a steady progression of structural change along the series with **1d** being the most distorted. Also, the NMR data[3a] indicate the uniqueness of **1a**, where in-plane distortion is most important, resulting in an opening of the bite angle of the ligand. This interpretation is consistent with the X-ray structure of $Ru(bpy)_2(\mathbf{1a})^{2+}$, which shows an N–Ru–N bite angle of 80.1° and a dihedral angle of 7.1° between the pyridine rings. The changing band patterns in the resonance Raman spectra (Figure 2) are indicative of the continuous structural variation in the coordinated ligand along the series **1b–d**.

The pattern of frequency shifts and intensity changes evident in Figure 2 may be interpreted with reference to the vibrational spectrum of biphenyl.[5g] In this comparison, the *xy* plane is the biphenyl molecular plane (D_{2h}), with the *x* axis along the inter-ring C–C′ bond. For chelated 2,2′-bipyridine (C_{2v}), *xz* is the molecular plane, with the *x* axis again along the inter-ring C–C′ bond. In this case, the biphenyl (D_{2h}) A_g and B_{2u} in-plane modes correlates as A_1 modes in C_{2v} and may be subject to resonance enhancement by excitation within a MLCT band. As previously demonstrated,[5g] the frequencies of biphenyl are recognizable in the resonance

Table II. Correlation of Ligand Modes (1000–1700 cm^{-1}) for Coordinated 2,2′-Bipyridine and Polymethylene-Bridged 2,2′-Bipyridines with Biphenyl Modes

sym (D_{2h})	biphenyl[a]	$Ru(bpy)_3^{2+}$ [b]	$Ru(\mathbf{1b})_3^{2+}$	$Ru(\mathbf{1c})_3^{2+}$	$Ru(\mathbf{1d})_3^{2+}$
A_g	1612	1607	1589	1581	1576
B_{2u}	1570	1563	1570	1569	1576
A_g	1507	1489	1480	1467	1468
B_{2u}	1432	1448[c]		1460 sh	1458
B_{2u}	1383			1434	1432
$-(CH_2)_n-$ C_3 ring			1336		1357
A_g	1285	1320	1318	1308	1297
B_{2u}	1272	1275	1267	1290	1297
A_g	1190	1173	1181	1185	1187
B_{2u}	1156	1109		1185	1171
B_{2u}	1074	1067[c]			
A_g	1030	1041[c]			
A_g	1003	1027			1035

[a] From ref 5g and 7. [b] Our frequencies in acetonitrile. [c] From ref 5h, observed with near-UV excitation.

Raman spectra of coordinated bipyridines. When coordinated 2,2′-bipyridine undergoes a twist about the inter-ring C_2–$C_{2'}$ bond, the symmetry drops to C_2 (possibly lower when ring nonplanarity is considered). Although some new totally symmetric modes would become Raman allowed, reference to biphenyl indicates that these out-of-plane (A_u and B_{2g}) modes (in D_{2h}) are below 1000 cm^{-1} and would not appear in spectra reported here. However, modes that were weakly enhanced (or even undetectable) for the more planar geometry may now show detectable enhancement as the ligand distorts from planarity. Frequency shifts accompany these intensity changes and may be due to bonding changes induced by a change in dihedral angle between the pyridine rings and/or changes in coupling between normal modes. Table II lists the detailed frequency correlations. With regard to intensity, for example, the coordinated bpy bands at 1607/1563 cm^{-1} (A_g/B_{2u} pair for biphenyl at 1612/1570 cm^{-1}) shift to 1570/1589 cm^{-1} for coordinated **1b** but maintain almost the same relative intensity. For coordinated **1c**, the 1569/1581-cm^{-1} pair have again shifted *and* reversed relative intensity.

It is evident, in a comparison of the $Ru(bpy)_3^{2+}$ spectrum with the spectrum of $Ru(\mathbf{1d})_3^{2+}$, that a significant redistribution of relative intensities has occurred. The bpy complex spectrum shows a strikingly dominant band at 1489 cm^{-1}, whereas the $Ru(\mathbf{1d})_3^{2+}$ spectrum shows three approximately equal intensity bands at 1576, 1468 (1458), and 1297 cm^{-1}. Examination of the intensities in the spectra of $Ru(\mathbf{1b})_3^{2+}$ and $Ru(\mathbf{1c})_3^{2+}$ shows that the change is continuous along the series. The existence of several equally intense bands in the spectrum of $Ru(\mathbf{1d})_3^{2+}$ indicates that there are several equally efficient Franck–Condon-Active vibrational modes in absorption. If the absorptive and emissive excited states are similar, the same normal modes would be active in coupling excited to ground states in emission. The 77 K emission spectrum (Figure 3) in each case shows a maximum for the 0–0 transition with a shoulder for the 1–0 transition, the separation of the maxima corresponding approximately to the frequency of the normal modes most efficient in coupling the excited to the ground state. $Ru(bpy)_3^{2+}$ shows a clearly defined low-frequency shoulder, consistent with a single mode being more prominent in coupling of the excited to the ground state. The spectra for the series of tris complexes with polymethylene-bridged bpy show progressively less well-defined low-frequency shoulders, as the bridge lengthens from **1b** to **1d**. This indicates that coupling is distributed more equally over a greater number of vibrational modes as the bridge length increases.

The measured lifetimes, both in solution at 25 °C and at 77 K (Table I), are remarkably similar for $Ru(bpy)_3^{2+}$ and for $Ru(\mathbf{1b})_3^{2+}$. Spectroscopic probes, including resonance Raman for the coordinated ligand, show that, in both cases, the bipyridines are similar and interact in a similar way with ruthenium(II). The similarities in their excited-state-related properties should not then be surprising. For the trimethylene-bridged complex in solution at 25 °C, the lifetime drops by about 30%, and at 77 K by about 50% (compared to $Ru(bpy)_3^{2+}$). The room-temperature solution emission is weaker by about 1 order of magnitude compared to that of the bpy or **1b** complexes. For $Ru(\mathbf{1d})_3^{2+}$ at 25 °C in solution, the emission is too weak to allow a lifetime measurement with our equipment, and at 77 K a large blue shift of the observed emission occurs and the lifetime is now rather close to that of $Ru(\mathbf{1c})_3^{2+}$. The similarities between the **1d** and the **1a** complexes with respect to emission properties have been previously discussed.[3a]

The large drop in quantum yield for emission from $Ru(\mathbf{1b})_3^{2+}$ to $Ru(\mathbf{1c})_3^{2+}$, with only a modest lowering of the measured lifetime, indicates that the nonradiative rate for deexcitation is much higher. Though we have no room-temperature lifetime for $Ru(\mathbf{1d})_3^{2+}$, we know that the quantum yield for emission is again approximately 1 order of magnitude less than for the trimethylene-bridged complex, again indicating a further increase in rate for nonradiative depopulation of the excited state. It has been shown[6] that the dominant "acceptor" modes in the nonradiative depopulation of excited states of bipyridine complexes are ring-stretching modes in the 1000–1700-cm^{-1} region. Furthermore, their relative involvement in this process is governed by the same type of consideration as the mechanism of resonance Raman intensity enhancement. Modes that show significant resonance enhancement for excitation within the MLCT band are predicted to be efficient in acting as "acceptor" modes for nonradiative deexcitation. The resonance Raman spectra reported here indicate that structural changes due to twisting along the C–C′ inter-ring bond lead to a situation in which more normal modes share more equally in providing overlap between the excited and ground states. These same modes are those capable of acting as "acceptor" modes and of depopulating the MLCT excited state via nonradiative processes.

Acknowledgment. This work was supported in part by the PSC-CUNY Research Award Program and the New York State Science and Technology Foundation (Grant No. SSF (85)-5). Support by the National Science Foundation is also acknowledged (Grant No. CHE-8511727 (H.D.G.) and CHE-8607935 (R.P. T.)).